Design of Composite Multilayer Surface Antenna Structure and Its Bending Fatigue Characteristics

Taechul Moon and Woonbong Hwang [*]

Department of Mechanical Engineering, Pohang University of Science and Technology,
San 31 Hyoja Dong, Namgu, Pohang, Kyungbuk, 790-784, Korea

Abstract

The present study aims to design a multilayer microstrip antenna with composite sandwich construction and investigate fatigue behavior of this multilayer SAS (surface antenna structure) that was asymmetric sandwich structure for the next generation of structural surface technology. This term, SAS, indicates that the structural surface becomes an antenna. Constituent materials were selected considering electrical properties, dielectric constant and tangent loss as well as mechanical properties. For the antenna performance, antenna elements inserted into structural layers were designed for satellite communication at a resonant frequency of 12.2 GHz. From electrical measurements, it was shown that antenna performances were in good agreement with design requirements. In cyclic 4-point bending, flexure behavior was investigated by static and fatigue test. Fatigue life curve of the SAS was obtained. The experimental results of bending fatigue were compared with single load level fatigue life prediction equations and in good agreement. The SAS concept is can be extended to give a useful guide for manufacturers of structural body panels as well as antenna designers.
© Koninklijke Brill NV, Leiden, 2008

1. Introduction

Communication areas will in the future be expanded by the use of satellite communication and satellite internet availability in vehicles. To implement these satellite services, especially in vehicles, antenna technology will be central. Antennas located on the surface of a structure take up much space, and suffer from large path-loss and junction-loss. In the past ten years, research has been performed on the embedding of antennas in load-bearing structural surfaces of aircraft in order to improve both structural efficiency and antenna performances: 'the structural surface becomes an antenna'. Structures, materials and antenna designers have recently

---

[*] To whom correspondence should be addressed. E-mail: whwang@postech.ac.kr
  Edited by KSCM

joined forces to develop a new high payoff technology called conformal load-bearing antenna structure or CLAS. The embedding of radio frequency antennas in a load-bearing structural surface is a new approach to the integration of antennas into structural body panels. It emerged from the need to improve structural efficiency and antenna performance. It demands integrated product development from disparate technologies, including structures, electronics, materials and manufacturing in order to generate a realistic design [1–3, 7].

The present study aims to design electrically and structurally effective antenna structures for future mobile communication, the next generation of structural surface technology. This is termed a surface antenna structure (SAS). Structurally effective materials with high electrical loss must not lower antenna efficiency in order to obtain both high electrical and mechanical performances. Design procedure is focused on high gain and wide bandwidth in the electrical part, and high strength, stiffness and environmental resistance in the mechanical part. A direct-feeding stacked microstrip patch antenna is used for the antenna performances and composite sandwich structure including composite laminates, and a Nomex honeycomb is applied to optimize mechanical performances. The basic structure is a composite sandwich that is very weight efficient; the core of the sandwich provides the necessary space for the antenna to function properly. Structural stability, including fatigue behavior and the fatigue life of SAS, will be estimated and predicted using the 4-point bending fatigue test.

2. Surface Antenna Structure and Materials

The fundamental design concept for the SAS panel is an organic composite multilayer sandwich panel in which mirostrip antenna elements are inserted, which means that the design idea is basically a composite sandwich structure mechanically and a microstrip antenna electrically, as shown in Fig. 1. Microstrip antennas can be used in high-performance aircraft, spacecraft, satellites and missile applications, where size, weight, cost, ease of installation, and aerodynamic profile are constraints. These antennas are low-profile, conformable to planar and nonplanar surfaces, simple and inexpensive to manufacture using modern printed-circuit technology and compatible with MMIC designs. One of the disadvantages of the original microstrip antenna configuration is narrow bandwidth. The conventional sandwich construction consists of two relatively dense and stiff facesheets that are bonded to either side of a low-density core. This helps to resist buckling of the facesheets under axial compressive loading, carry bending-induced axial loads and improve fatigue characteristics. As shown in Fig. 2, the basic panel layers are two facesheets, two honeycomb cores and antenna elements on dielectrics.

The facesheet and supporter mechanically carry a significant portion of the in-plane loads, contribute to overall panel buckling resistance, and provide low velocity impact and environmental resistance, while the outer facesheet that is placed above the radiating patch electrically provides signal loss by its high electrical loss
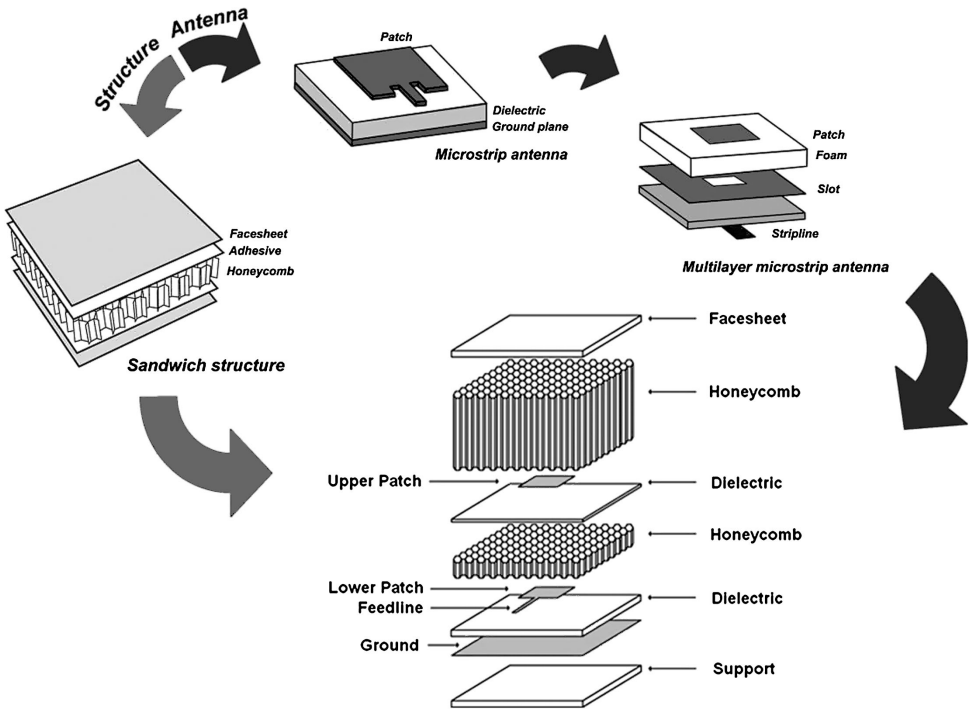
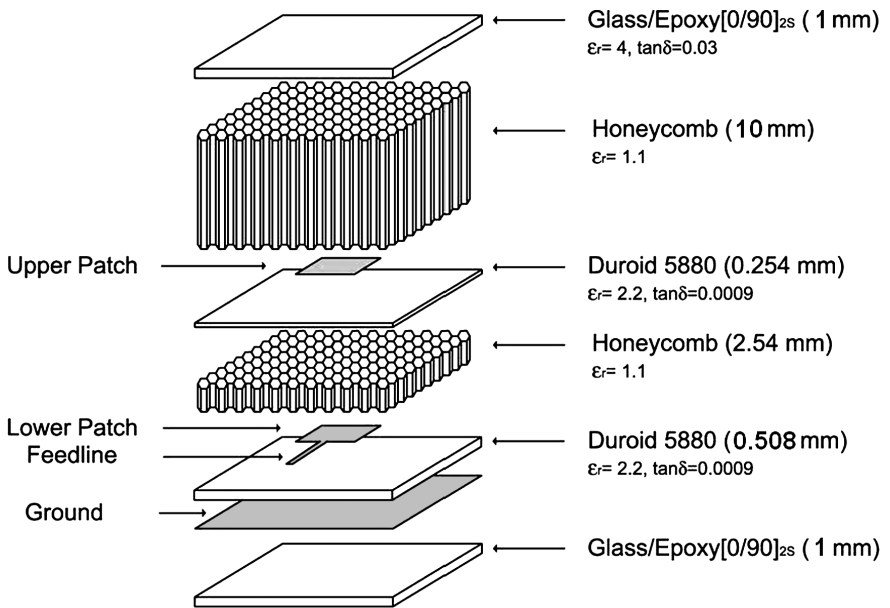**Figure 1.** Basic concept of the surface antenna structure (SAS).

Figure 2. Geometry of a composite surface antenna structure (SAS).

Table 1.
Electrical and mechanical properties of constituent materials in SAS

Materials	Properties
Woven glass/thermosetting plastic (RT duroid 5880 Rogers co.)	Elastic modulus: 1.07 GPa Tensile strength: 29 MPa Dielectric constant: 2.2 Loss tangent: 0.0009
Glass/epoxy $[0/90]_{2s}$	Elastic modules: 25.4 GPa Tensile strength: 573.6 MPa
Nomex Honeycomb (Hexel co.) 10 mm 10–1/8–5	Compressive modulus: 5.31 MPa Compressive strength: 255 MPa Shear strength: 70.3 MPa Dielectric constant: 1.1
Nomex Honeycomb (Hexel co.) 2.54 mm 10–1/8–6	Compressive modulus: 7.76 MPa Compressive strength: 414 MPa Shear strength: 88.6 MPa Dielectric constant: 1.1

(loss tangent) when the signal passes through it. However, it can make antenna radiate more efficiently without electrical loss when it is placed at the resonance position [7].

The honeycomb cores mechanically transmit shear load induced from bending loads in the panel, support the outer facesheet against compression wrinkling, provide impact resistance and increase the overall panel buckling resistance; they electrically provide an air gap without signal loss and the position of the outer facesheet is adjusted for maximum antenna performance. The thicknesses of honeycomb cores contribute to antenna efficiency as well as the overall rigidity.

The upper patch and lower patch are separated by an air gap that is provided by the honeycomb of 2.54 mm thickness. Duroid 5880 used for layers of antenna elements has good electrical properties of low dielectric constant and electrical loss, but it does not contribute to structural performances. Electrical and mechanical properties of materials composed of SAS are given in Table 1.

The designed antenna elements with their dimensions are shown in Fig. 3. The upper radiating patch is smaller than the lower patch and the impedance at the central edge of the lower patch is 100 Ω, which is transformed to 50 Ω feedline. To improve the narrow bandwidth problem with the original microstrip antenna configuration, two-stacked radiating patches are used to provide a wide bandwidth, which is made by coupling of the dual resonance system. In the design procedure, antenna performances are aimed for Ku-band satellite communication, frequency range from 11.7 to 12.75 GHz with linear polarization. Computer-aided design tool (Ansoft Ensemble 6) is used to select a large number of strongly interacting parameters by integrated full-wave electromagnetic simulation.
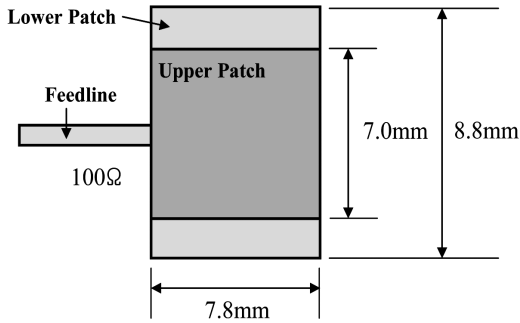
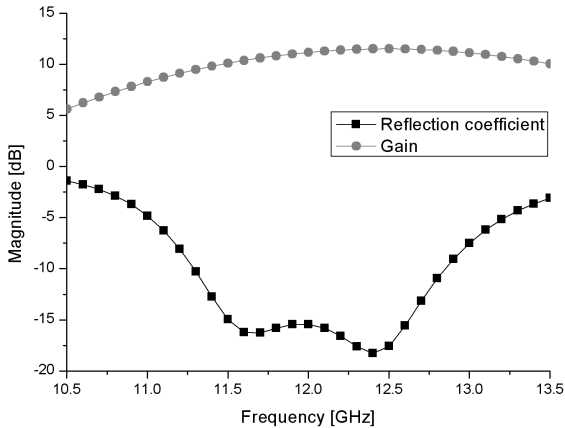**Figure 3.** Designed antenna elements with stacked patches.

**Figure 4.** Reflection coefficient and gain of SAS.

In the design procedure, the optimized thicknesses of the outer facesheet and honeycomb are respectively selected as 1 and 10 mm, in which structure maximum gain is obtained by the resonance condition and a wide bandwidth is also achieved at 10 mm by using stacked radiating patches. Figure 4 shows the reflection coefficient and the gain of SAS. It resonates at the central frequency of 12.4 GHz, frequency range from 11.3 to 12.8 GHz with linear polarization. This is also satisfied in the desired frequency range with bandwidth of 1.5 GHz at VSWR 2. The gain is higher by 2.3 dBi, with the outer facesheet (11.55 dBi), compared with that of the antenna without the facesheet (9.25 dBi).

3. Structural Experiments

The symmetric sandwich structure (Facesheet, Core material, Facesheet) has been intensively investigated both experimentally and theoretically, but the present SAS has an asymmetric sandwich structure. We now investigate experimentally the flexural behavior of this asymmetric sandwich structure based on 4-point static and
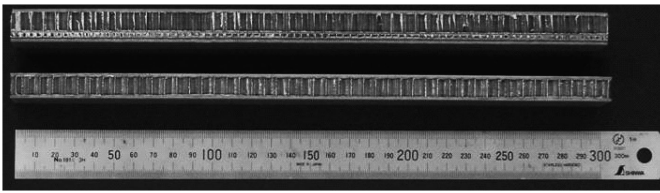
(a)
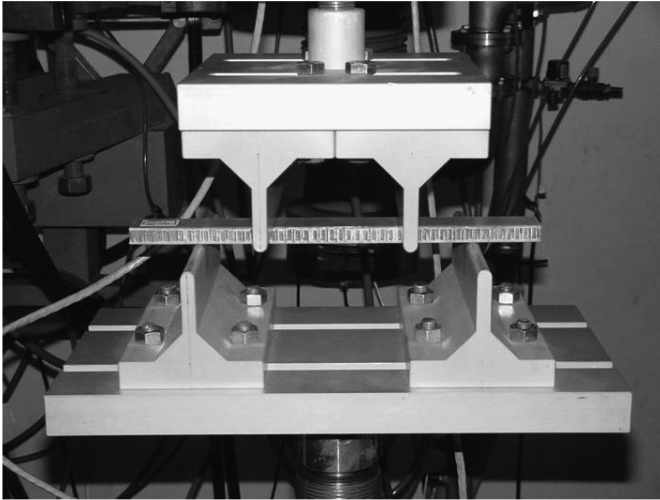
(b)

Figure 5. (a) Test specimens 300 (mm) × 30 (mm). (b) Configuration specimen and jig.

fatigue testing, so as to predict the fatigue life experimentally, and we compare these results with theoretical predictions.

3.1. Experimental Procedure

The static 4-point bending test, in accordance with ASTM C 393-62 [4], and the 4-point bending fatigue test were performed using MTS 458 material testing system to find the mechanical properties of the SAS. The specimen was supported by a quarter point-loading jig as shown in Fig. 5. The upper specimen of Fig. 5(a) is the present asymmetric sandwich structure and the lower specimen is the symmetric sandwich structure. Static bending tests were performed under displacement-control at a cross-head speed 1 mm/min until failure occurred. The fatigue tests were performed under load-control using a sinusoidal wave form applied at frequency of 1 Hz, which should cause only negligible temperature increase during testing, and were carried out to the life-time limit of 10^6 cycles. This 10^6 cycle limit was chosen to be representative of the industrial reference for fatigue tests performed on such shapes. The failure criterion in the fatigue test was chosen according to the maximum deflection obtained from static tests. Applied load levels were determined at 0.9–0.6 load levels for the static bending test. Three test speci-
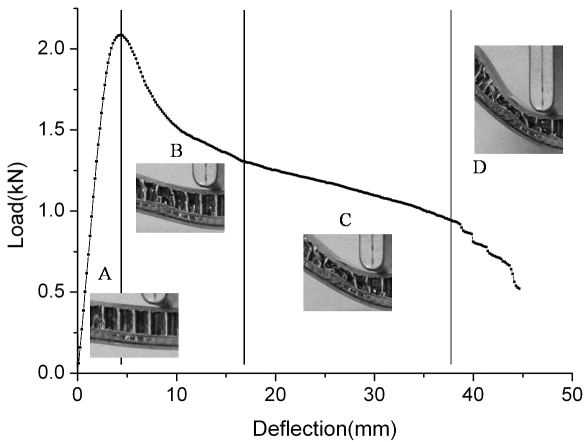
Figure 6. Static flexural behavior of SAS.

mens were used for each load level. All tests were conducted at room temperature under laboratory conditions.

3.2. Results and Discussion

Figure 6 shows the displacement–load curve from static test. The displacement–load curve can be divided four regions denoted by A, B, C and D, since the SAS consists of elements of sandwich structure and has multilayer of facesheets, honeycombs, and two antenna elements with dielectrics. Damage development was as follows.

  I. Region A: deflection propagates linearly through the entire specimen. Then, at the transition point between regions A and B, failure sheet begins.

 II. Region B: after the failure of the facesheets, the deflection again propagates linearly. Then, the failure of honeycomb and antenna elements with dielectrics occurs.

III. Region C: after the deflection propagates, the shear failure of both honeycombs occurs.

IV. Region D: all of the SAS fails completely with delamination.

   Face failure and core wrinkling were observed in all specimens, as a result of the asymmetry between the top and bottom faces. At final failure, the bending load of the SAS was 2.09 kN, and the bending displacement was 4.5 mm. The flexural behavior of the SAS was followed mode B (Core shear) of the Ashby and colleagues [5].

   Figure 7 shows the resulting displacements at the load level of 0.8. This result shows a continuing increase of both the resultant and permanent displacement with the number of cycles. This suggests that the sandwich structure of the SAS might undergo continual degradation from the early stage of loading until failure. The
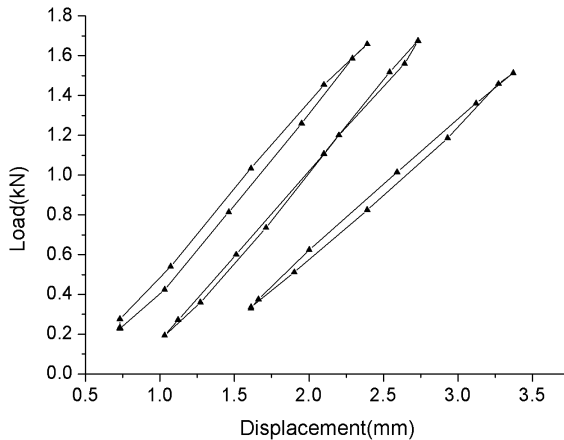
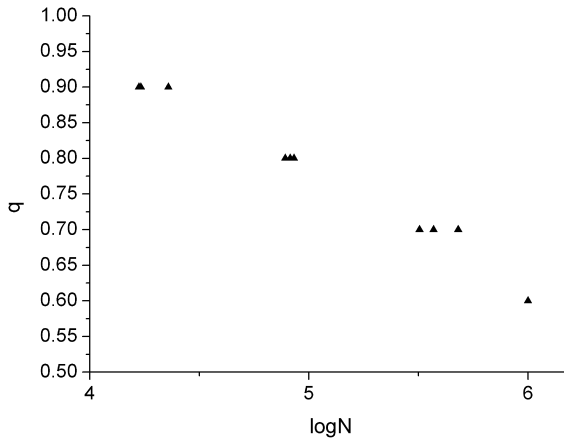**Figure 7.** Cyclic load–displacement behavior of SAS at load level 0.8.

Figure 8. Fatigue life data of SAS.

displacements increase faster at higher loads than at lower loads. The rate of increase of both resultant and permanent displacements, d (displacement), dn (cycle), decreases with the number of cycles in the early stage of fatigue, and increased drastically during the final few cycles. Also, the hysteresis loop energy decreases after the first cycle as far as a certain number of cycles, and increases rapidly during the final stages. After failure, the resultant displacements of the SAS were 4.1 mm, which is less than 4.5 mm from the static bending test. This result confirms Hwang *et al.*'s failure criterion [6] that the failure of composites under fatigue loading occurs when the fatigue resultant displacement reaches a specific multiple of the static ultimate displacement. Figure 8 shows the log scale relation of load levels (ratio of applied load and bending load) and fatigue cycles. The test results show that SAS can support external loads as a structural surface while giving excellent antenna performance.

Using the flexure test results, we compared various Single Load Level Fatigue Life Prediction Equations (SFLPEs) with the experimental data. The SFLPEs to be compared were Hwang *et al.*'s equation, Basquin's relation and S–N Curve:

$$\text{Hwang } et\ al.\text{'s equation: } N = [M(j^{B} - q^{B})]^{1/C}, \tag{1}$$

$$\text{Basquin's relation: } \sigma_{a} = \sigma'_{f}(2N)^{b}, \tag{2}$$

$$\text{S–N curve: } q = k \log N + d, \tag{3}$$

where N is the fatigue life, σ_{a} is the applied load, q is the applied load level and k, d, σ'_{f}, and b are material constants.

The test results and commercial software Origin 7.5 was used to estimate these parameters from our data. The results are as follows:

$$\text{Hwang } et\ al.\text{'s equation: } N = \left[\frac{0.6308^{-7.516}}{-0.0001832}(0.9111^{-7.516} - q^{-7.516})\right]^{-1/1.1519}, \tag{4}$$

$$\text{Basquin's relation: } \sigma_{a} = 482.4396(2N)^{-0.09287}, \tag{5}$$

$$\text{S–N curve: } q = -0.15912 \log N + 1.57628. \tag{6}$$

Figure 9 shows that experimental results were compared with single load level fatigue life prediction equations and are in especially good agreement with Hwang *et al.*'s equation.

4. Conclusions

The surface antenna structure (SAS) was designed with structurally effective materials without compromise with electrical properties. SAS is a composite sandwich structure in which a microstrip antenna is placed between a honeycomb core and a lower facesheet. SASs having both high electrical and mechanical performances
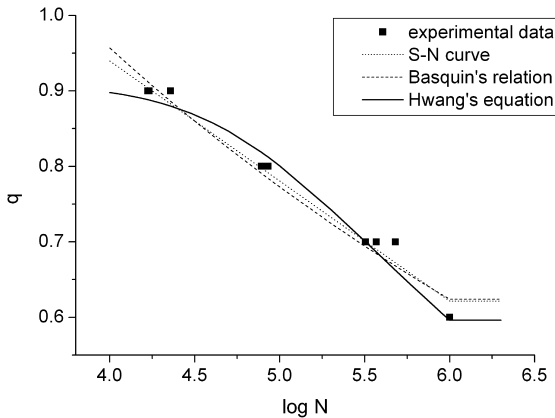

Figure 9. Fatigue life prediction curves.

are designed for requirements of satellite communication. Bending characteristics under static loading were investigated, and flexural behaviors of cyclic loading were studied using a 4-point bending fatigue test. The test results were compared with SFLPEs and good agreement was found. The SAS concept makes it possible to design the antenna structure with structurally effective materials for the communicative body panel in the vehicles and can be extended to give a useful guide for manufacturers of structural body panels as well as antenna designers, promising future communication technology.

References

1. A. J. Lockyer, J. N. Kudva, D. Kane, B. P. Hill, C. A. Martin, A. C. Goetz and J. Tuss, A qualitative assessment of smart skins and avionics/structures integration, *SPIE Smart Struct. Mater.: Smart Mater.* **2189**, 172–183 (1994).
2. J. Truss, A. Lockyer, K. Alt, F. Uldrich, R. Kinslow, J. Kudva and A. Goetz, Conformal load bearing antenna structures (CLAS), in: *37th AIAA SDM Conf.*, Salt Lake City, USA, pp. 836–843 (1996).
3. A. J. Lockyer, K. H. Alt, D. P. Coughlin, M. D. Durham, J. N. Kudva, A. C. Goetz and J. Tuss, Design and development of a conformal load-bearing smart-skin antenna: overview of the AFRL smart skin structures technology demonstration (S3TD), *SPIE Conf. Industr. Comm. Appl. Smart Struct. Technol.* **20**, 125–153 (1999).
4. *ASTM*, 15.03, **C393**, 22–24 (1992).
5. A.-M. Harte, N. A. Fleck and M. F. Ashby, The fatigue strength of sandwich beams with an aluminium alloy foam core, *Intl. J. Fatigue* **23**, 499–507 (2001).
6. W. Hwang, C. S. Lee, H. C. Park and K. S. Han, Single- and multi-stress level fatigue life of prediction of glass/epoxy composites, *J. Adv. Mater.* **26**, 3–9 (1995).
7. C. S. You and W. Hwang, Multilayer surface-antenna-structure for Ku-band satellite communication, in: *14th Intl. Conf. Adaptive Struct. Technol.*, Seoul, Korea, October (2003).
8. D. H. Kim, W. Hwang, H. C. Park and W. S. Park, Fatigue characteristics of surface antenna structure designed for satellite communication, *J. Reinf. Plast. Compos.* **24**, 35–51 (2005).
9. C. S. You and W. Hwang, Design and fabrication of composite-smart-structures having high electrical and mechanical performances for future mobile communication, *Mech. Compos. Mater.* **40**, 237–246 (2004).